Polymer 49 (2008) 4889–4898

Contents lists available at ScienceDirect

Polymer

journal homepage: www.elsevier.com/locate/polymer

Phase behavior in liquid crystallization for diblock copolymers consisting of rubbery amorphous and side-chain liquid crystalline components

Shin-ichi Taniguchi [a], Hiroki Takeshita [a], Mitsuo Arimoto [a], Masamitsu Miya [a], Katsuhiko Takenaka [a,b], Tomoo Shiomi [a,b,*]

[a] Department of Materials Science and Technology, Nagaoka University of Technology, Japan
[b] Center for Green-Tech Development in Asia, Nagaoka University of Technology, 1603-1 Kamitomioka, Nagaoka, Niigata 940-2188, Japan

ARTICLE INFO

Article history:
Received 2 May 2008
Received in revised form 19 August 2008
Accepted 26 August 2008
Available online 13 September 2008

Keywords:
Liquid crystalline block copolymer
Liquid crystallization process
Microphase separation

ABSTRACT

Phase behavior in liquid crystallization was studied for a series of liquid crystalline (LC) diblock copolymers consisting of rubbery amorphous and side-chain liquid crystalline components, poly(*n*-butyl acrylate) (PBA) and poly[11-(4′-cyanophenyl-4″-phenoxy)undecyl acrylate] (PLC), respectively, using a time-resolved small-angle X-ray scattering (SAXS) techniques, DSC and polarized optical microscopy (POM). The block copolymers used had three kinds of copolymer compositions, 44, 20 and 15 wt% of PLC compositions (BLC44, BLC20 and BLC15, respectively). BLC44 showed a smectic liquid crystalline structure. In the process of liquid crystallization for BLC44, the SAXS peak due to the microphase separation structure existing before liquid crystallization was changed continuously to be at a smaller angular side, and at almost the same time, a new peak appeared at a further smaller angular side and developed. The former peak disappeared with the development of liquid crystallization. The behavior of these SAXS peaks suggests that the microphase separation structure was changed discretely at the transition from isotropic to smectic and that two phases coexist in the early stage of the liquid crystallization. The coexistence of two peaks in the early stage of the liquid crystallization corresponded to the POM observation. In the isotropization process, coexistence of two phases was not observed. For BLC20 exhibiting a cylindrical structure in both isotropic and liquid crystalline states, the liquid crystalline structure was not smectic but probably nematic, and the spacing was changed continuously in liquid crystallization. No liquid crystallization was observed in SAXS, POM and DSC for BLC15. The orientation of smectic layers within lamellar domains was investigated using 2D-SAXS images. The smectic layer was aligned perpendicularly to the lamellar interface.

© 2008 Elsevier Ltd. All rights reserved.

1. Introduction

Block copolymers containing a side-group liquid crystalline (LC) block have a potential to exhibit hierarchical phase structure or ordering. The hierarchical structure in liquid crystalline block copolymers consists of several ten nanometers of microphase separation structure and a few nanometers of liquid crystalline structure. Such superimposed structure has been studied extensively [1–17]. The orientation of mesogenic groups or smectic (Sm) layers within microphase domains has mainly been focused on so far [7–17]. Namely, a main subject has been concerning whether the mesogens or Sm layers are aligned perpendicular or parallel to the interface between the domains of two blocks in various microphase separation structures.

On the other hand, there are a very few reports on changes of microphase separation structure or its size in liquid crystallization from microphase-separated states [10]. For crystalline–amorphous block copolymers, many investigations on the structural change in crystallization have been reported [18]. The microphase separation structure is not changed for block copolymers having a glassy amorphous block [19–21], while it can be changed for block copolymers containing a rubbery component because rubbery polymer chains can move flexibly during crystallization [22–24]. It has been reported that such structure change depends on competition between crystallization and chain diffusion rates as well as segregation degrees of microphase separation. For liquid crystalline block copolymers, on the other hand, Li et al. found a continuous decrease in lamellar spacing of the microphase separation structure at the transition from nematic to isotropic state [10]. There may be a very few investigations on such structure change in liquid

* Corresponding author. Center for Green-Tech Development in Asia, Nagaoka University of Technology, 1603-1 Kamitomioka, Nagaoka, Niigata 940-2188, Japan. Tel.: +81 258 47 9304; fax: +81 258 47 9300.
E-mail address: shiomi@vos.nagaokaut.ac.jp (T. Shiomi).

0032-3861/$ – see front matter © 2008 Elsevier Ltd. All rights reserved.
doi:10.1016/j.polymer.2008.08.060

Table 1
Characteristics of block copolymers and PLC homopolymer

Code	M_n		LC/wt%	M_w/M_n[c]
	PBA[a]	PLC[b]		
PLC	–	3000[c]	–	1.11
BLC44	37 900	30 000	44	1.21
BLC20	34 000	8200	20	1.04
BLC15	37 900	6900	15	1.12
BLC51	15 000	15 400	51	1.20

[a] Determined in THF at 40 °C using SEC with a light scattering detector.
[b] Determined from copolymer composition measured by ^{1}H NMR on the basis of molecular weight of PBA.
[c] Determined by SEC using standard poly(styrene).

crystallization. Also, it is not clear whether the change is continuous or discontinuous.

In this paper, we will present changes of microphase separation structure in liquid crystallization from microphase-separated isotropic states for block copolymers consisting of rubbery amorphous and side-group liquid crystalline blocks. The orientation of mesogenic groups or Sm layers within the microdomain will also be discussed.

2. Experimental

2.1. Materials

Poly[11-(4′-cyanophenyl-4″-phenoxy)undecyl acrylate] homopolymers (PLC) and block copolymers (BLC) composed of PLC and poly(*n*-butyl acrylate) (PBA) were prepared by atom transfer radical polymerization (ATRP). Synthesis of LC monomers and their polymerization for PLC homopolymer were performed according to the method of Kasko et al. [3,5] In homopolymerization of LC, 11-(4′-cyanophenyl-4″-phenoxy)undecyl 2-bromopropionate was employed as an initiator. As a Cu-solubilizing ligand, 4,4′-dinonyl-2,2′-dipyridyl (bpy9) was used instead of 4,4′-diheptyl-2,2′-dipyridyl (bpy7) used by them. Li et al. also used bpy9 [10]. The polymerization was performed for 3 h at 110 °C. The resulting polymers were purified by reprecipitating three times

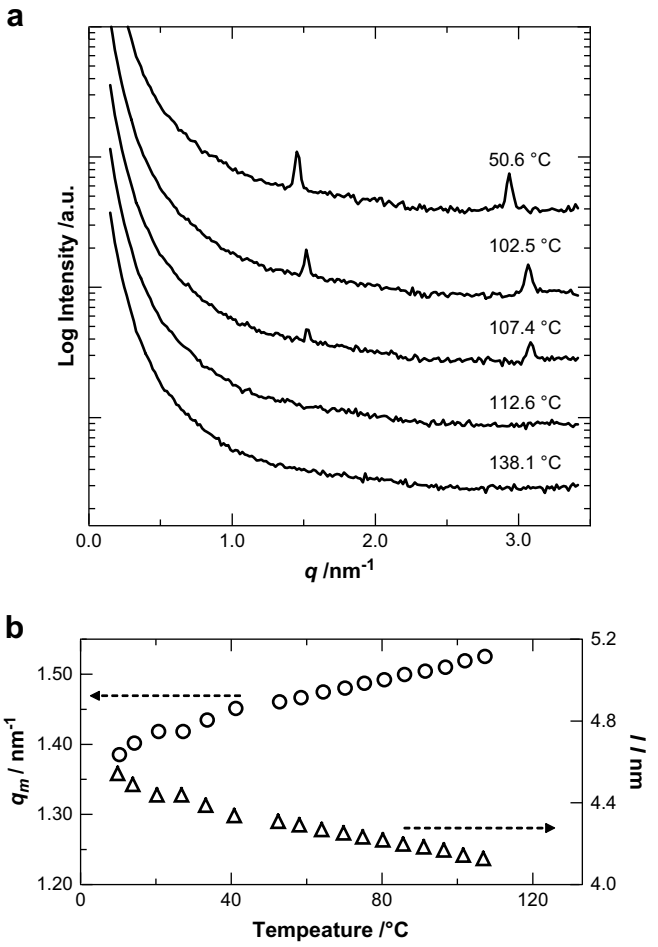

Fig. 2. SAXS profiles at each temperature in heating of 10 °C/min (a) and temperature dependences of the first-order peak position q_m and the spacing l in Sm structure (b) for PLC homopolymer.

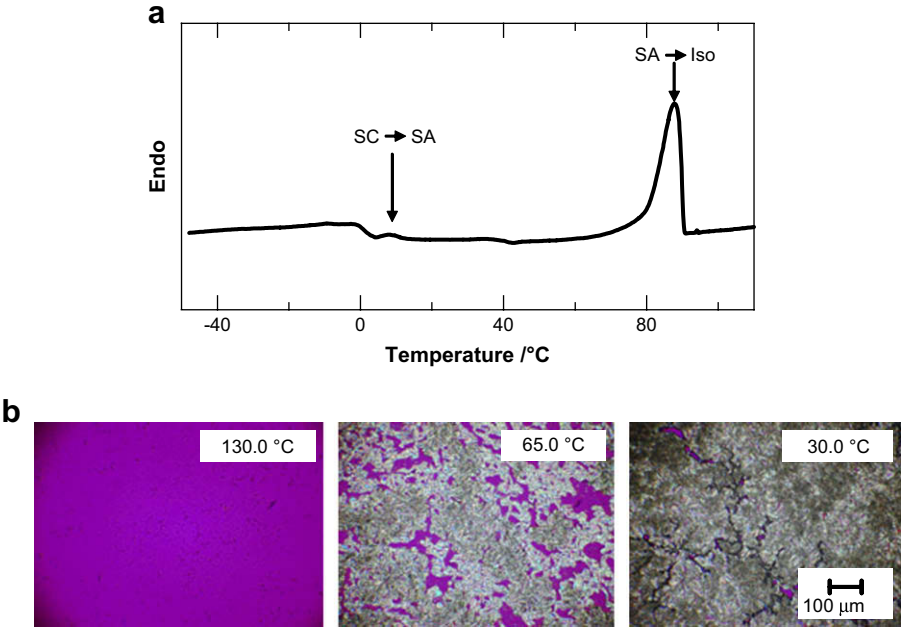

Fig. 1. DSC thermogram in heating (a) and POM pictures at cooling rate of 4 °C/min (b) for PLC homopolymer.

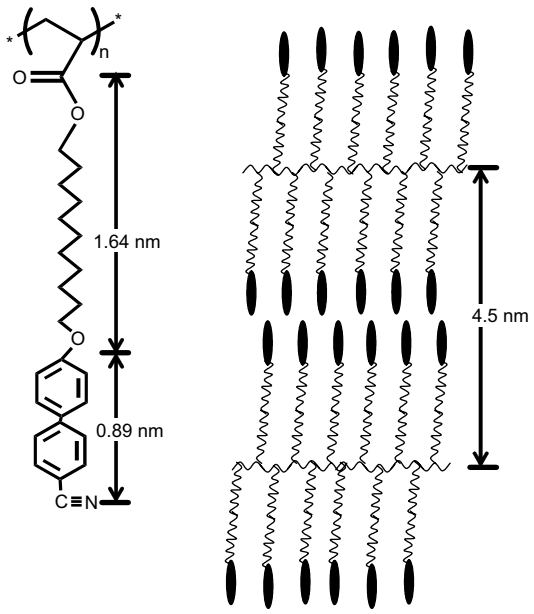

Fig. 3. Bilayer smectic structure.

with a THF/methanol system to remove unreacted monomer, CuBr and bpy9, followed by drying under vacuum. Block copolymers were prepared by ATRP of LC monomers using a PBA macroinitiator synthesized by ATRP. Bpy9 was used as the ligand in both polymerizations for PBA macroinitiator and BLC. The polymerization for PBA initiator was carried out for 3 h at 110 °C, and the resulting product was purified by reprecipitation method with a THF/−50 °C methanol system. BLC block copolymers were purified with a THF/methanol system, followed by drying under vacuum.

2.2. Characterization

Absolute molecular weights of PBA macroinitiator were measured by Size Exclusion Chromatography (SEC) using a TOSOH HLC-8220 instrument equipped with a Viscotek model 270 dual detector with a low-angle light scattering detector. The molecular weight of PLC homopolymer was determined by SEC (TOSOH HLC-8020 instrument equipped with an RI detector). A solvent used in SEC measurements was THF. Copolymer compositions of BLC were determined by 400 MHz ^{1}H NMR in $CDCl_3$ with a JEOL JNM-GX400 spectrometer. Molecular weights of BLC block copolymers were estimated from the copolymer composition on the basis of the

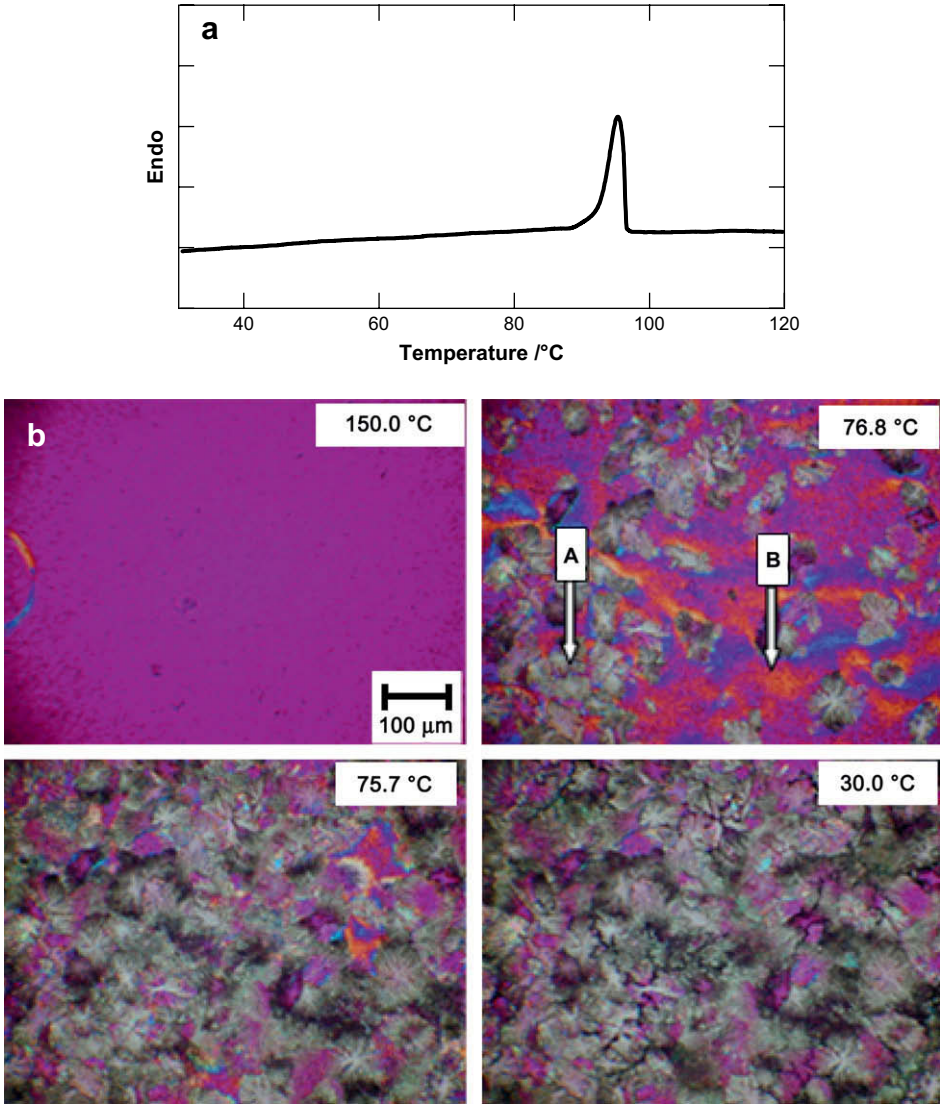

Fig. 4. DSC thermogram in heating (a) and POM pictures in cooling of 4 °C/min (b) for BLC44. In (b), A and B indicate fan-like structure and yellow/blue area, respectively.

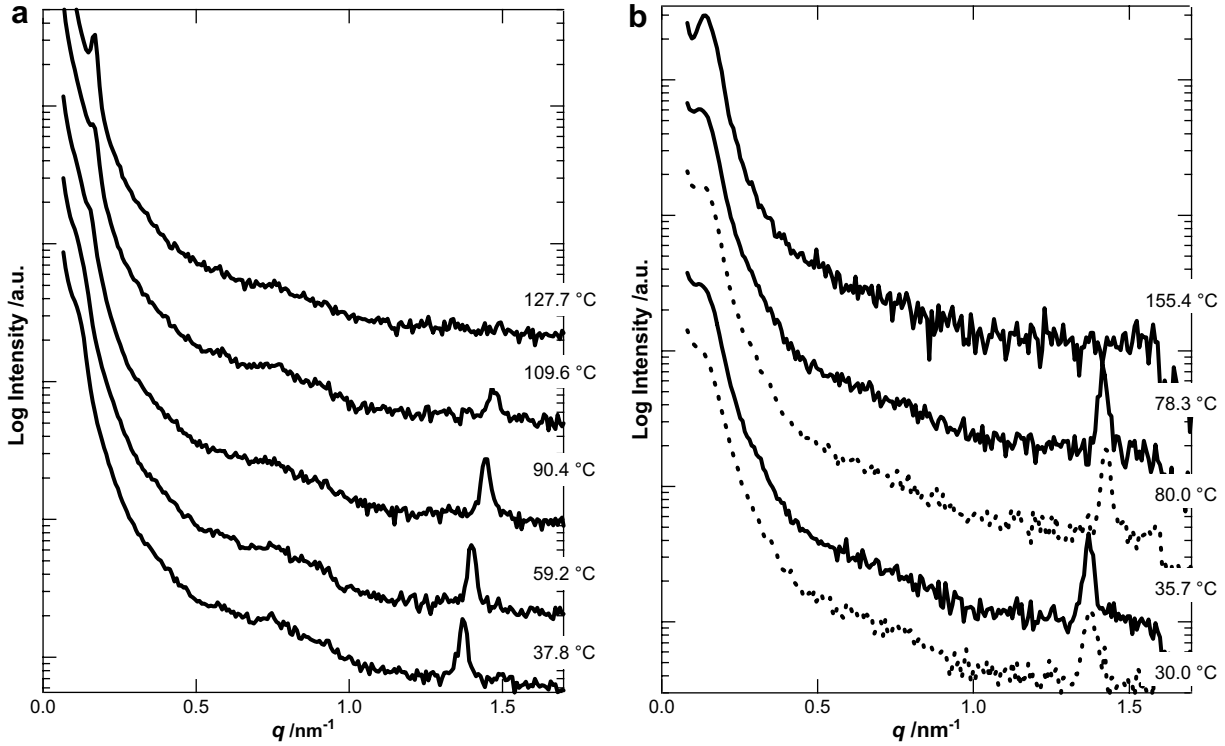

Fig. 5. (a) SAXS profiles in cooling at 4 °C/min for BLC44. (b) SAXS profiles at indicated temperatures in cooling at 4 °C/min (solid line) and in quenching rapidly to indicated temperatures from the isotropic state at 155.4 °C (dotted line) for BLC51.

molecular weight of PBA macroinitiator. Polydispersity of molecular weights was determined by SEC with the RI detector.

Characteristics of PLC homopolymer and BLC block copolymers are shown in Table 1.

2.3. Sample preparation and measurements

The polymer was dissolved in THF to be a 5 wt% solution, and then dried at room temperature overnight, followed by removing the solvent completely in a vacuum oven at 60 °C overnight.

Structures of microphase separation and liquid crystals were observed using time-resolved Small-Angle X-ray Scattering (SAXS) employing synchrotron radiation. SAXS measurements were performed using beam lines BL-10C and BL-15A for 1D and 2D experiments, respectively, at the Photon Factory in the Institute of Materials Structure Science, High Energy Accelerator Research Organization in Tsukuba, Japan. Details of optics and instrumentation for 1D measurements were described elsewhere [25]. The scattering images in 2D experiments were collected by a CCD camera (C4880, Hamamatsu Photonics K.K.) with an image intensifier. The scattering vector was defined as $q = (4\pi/\lambda)\sin(\theta/2)$, where θ is the scattering angle. The scattering angle was calibrated by using a chicken tendon having periodical structure of 65.3 nm. 1D time-resolved SAXS measurements were performed in heating

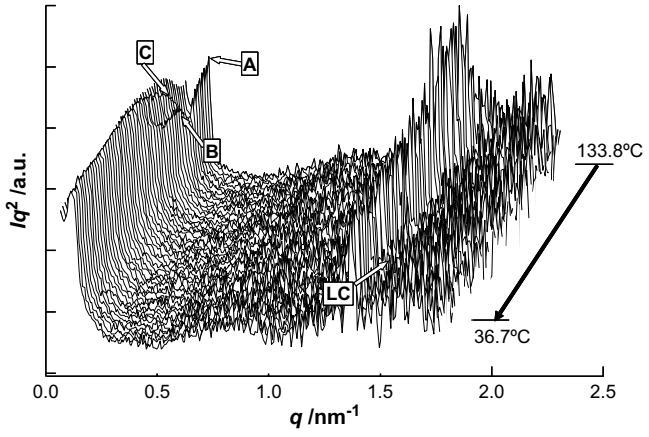

Fig. 6. Development of Lorentz-corrected SAXS profile for BLC44. The peaks A–C are due to the microphase separation structure, and the peak LC due to Sm layers.

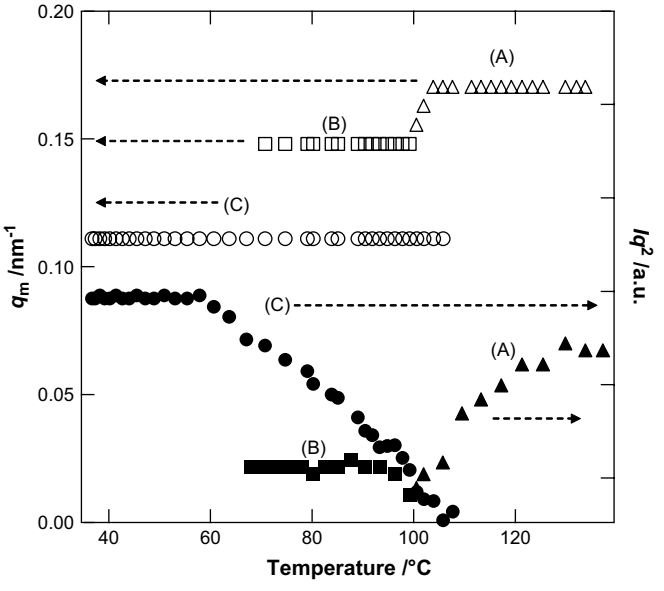

Fig. 7. Changes of the peak position q_m (open symbols) and its intensity Iq^2 (filled symbols) in cooling process at 4 °C/min for BLC44. A–C correspond to the respective peaks shown in Fig. 6.

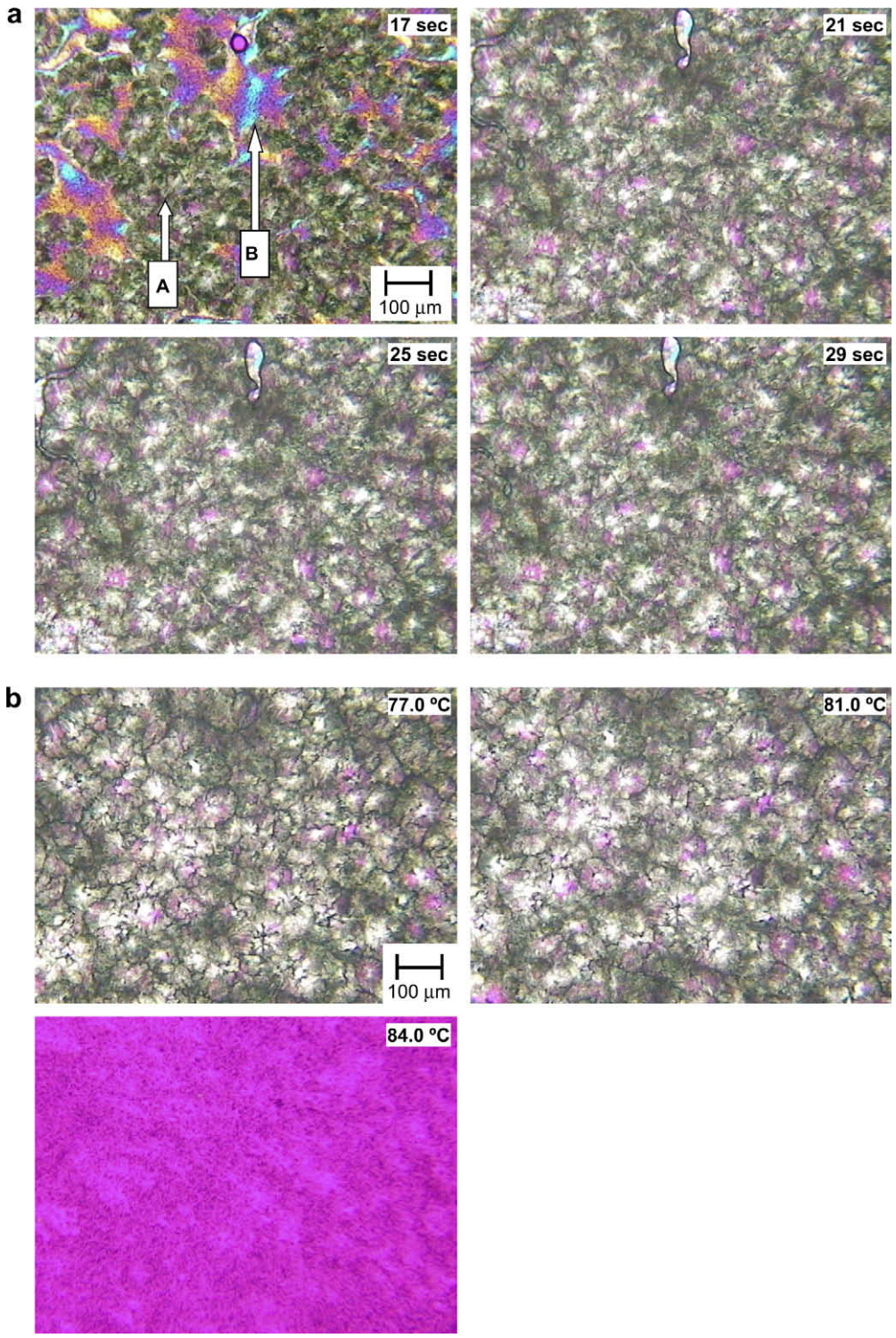

Fig. 8. POM pictures in quenching to 77.0 °C from the isotropic state (a) and in the heating process after that (b).

or cooling in the range of 30–160 °C. In isothermal measurements, the sample was annealed at 160 °C for 30 min and then moved rapidly into a measurement holder thermostated at a desired temperature. In 2D experiments, oscillating shear flow was applied to the 100-μm-thick sample at 1 Hz and 80 °C for 20 min using a Linkam CSS-450 apparatus just before SAXS measurements, where the sample was sandwiched between two stainless plates with X-ray windows made of polyimide films.

A Perkin Elmer Pyris 1 apparatus was used for DSC measurements. The sample annealed at 150 °C for 10 min in a sample pan was cooled at 4 °C/min and then heated at 4 °C/min.

For observation by Polarized Optical Microscopy (POM), an Olympus BH-2 microscope equipped with a Nicon Coolpix 950 digital camera was used. The temperature was controlled with a Mettler FP82HT hot stage running through an FP90 central processor.

3. Results and discussion

3.1. Liquid crystalline structure of PLC homopolymer

Two transition temperatures for PLC homopolymer are observed in the DSC thermogram of Fig. 1a as follows: 8.3 and 87.9 °C. These transitions can be assigned to be smectic C–smectic A and smectic A–isotropic, respectively, according to Kasko et al. [5]. They obtained the molecular weight dependence of these transition temperatures for the same liquid crystalline polymers. The above temperatures obtained here are almost the same as those by them for the polymers with the corresponding molecular weight. The enthalpy ΔH_t of the smectic A–isotropic transition is 6.6 J/g (2.8 kJ/monomer mol), which is almost the same as that reported by Kostromin and Shibaev [26]. Fig. 1b shows POM pictures, which exhibit the liquid crystallization below the isotropization temperature T_{iso} observed by DSC.

Fig. 2a shows SAXS profiles for PLC homopolymer at each temperature in the heating process. Two peaks can be observed below T_{iso}. The ratio of these peak positions is 1:2, which means layer structure, that is, smectic structure Sm. The layer spacing l is estimated from the first-order peak position around $q = 1.4\ nm^{-1}$ to be about 4.5 nm. Kostromin and Shibaev also reported l to be 4.4 nm for the same liquid crystalline polymer [26]. This value of the layer spacing is about twice the length of the side group with the mesogen and *trans* zigzag conformation of $(CH_2)_{11}$, which suggests that the smectic structure is a bilayer structure consisting of two mesogenic layers as shown in Fig. 3. Such a bilayer structure has been reported for liquid crystalline polymers having cyanobiphenyl mesogens [9,26]. As shown in Fig. 2b, the peak positions due to Sm layer shift to a smaller q with decreasing temperature, namely the spacing l of the Sm layer varies from 4.1 to 4.5 nm in the range of 107–10 °C. Usually the mesogen axis may become tilted more against the Sm layer with decreasing temperature so that l becomes smaller. The result obtained here shows the opposite trend. In the present stage, it is not clear what change occurs in liquid crystalline structure.

3.2. Phase behavior in liquid crystallization of block copolymers

Fig. 4a shows DSC thermograms in the heating process for BLC44 block copolymer. T_{iso} is not so different from that of PLC homopolymer in spite of the higher molecular weight of LC block than that for the PLC homopolymer, while $\Delta H_t (= 5.8\ J/g)$ is somewhat smaller than that for the homopolymer. The liquid crystallization is observed below T_{iso} in POM pictures shown in Fig. 4b.

The SAXS profiles of BLC44 in cooling from 150 to 30 °C are shown in Fig. 5a. In the isotropic state (127.7 °C), a peak due to microphase separation structure is observed at $q = 0.17\ nm^{-1}$. Although any higher-order peaks are not clearly observed, microphase structure is considered to be lamellar by taking account of the copolymer composition. A peak due to Sm layers appears around $q = 1.4\ nm^{-1}$ below about 100 °C together with its second-order peak at $q = 2.8\ nm^{-1}$ (in which the second-order peak is not shown in Fig. 5a because it is beyond the q range indicated here). The position of the peak due to the Sm layer shifts to a smaller q with decreasing temperature in the same way as that for the PLC homopolymer. This temperature dependence of the peak position can be reconfirmed in the SAXS profiles shown in Fig. 5b, which shows comparison of the SAXS profiles between the cooling process and on quenching rapidly the samples from the isotropic state to the indicated temperatures. The peak positions in these two situations are the same as each other at the respective temperatures. Therefore, the shift of q due to the Sm layer does not occur in the process of liquid crystallization but depends on the temperature.

In order to observe in detail a change of the microphase separation structure in the liquid crystallization process, the development of Lorentz-corrected SAXS profiles for BLC44 is shown in Fig. 6. As a peak due to Sm layers appears at $q = 1.4\ nm^{-1}$, the intensity of a preexisting peak around $q = 0.17\ nm^{-1}$ (indicated by 'A' in Fig. 6) above T_{iso} decreases and the peak is succeeded by peak 'B'. Furthermore, at almost the same time a new peak ('C') appears and develops at a smaller angular side. Peak B disappears with development of peak C. Peak C may come from the microphase separation structure containing Sm LC layers because the peak due to the Sm layer exists in the whole temperature range below T_{iso}, although the liquid crystalline structure related to peak B is obscure. The position q_m and intensity Iq^2 of these peaks due to the microphase separation structures are plotted against the temperature in Fig. 7. The peak position q_m is changed from $q_m = 0.17\ nm^{-1}$ in the isotropic state to about 0.15 and $0.11\ nm^{-1}$ with liquid crystallization around 100 °C, and finally only the peak at $q_m = 0.11\ nm^{-1}$ remains. These values of q_m correspond to the spacing $d = 38$, 42 and 56 nm, respectively.

As shown in Figs. 6 and 7, the change from $q_m = 0.17$ to $0.15\ nm^{-1}$ appears to be continuous, while the change from $q_m = 0.17$ to $0.11\ nm^{-1}$ is discrete. The discrete change means that the microphase separation structure is reorganized by liquid crystallization. Furthermore, the coexistence of two q_ms at 100–70 °C suggests that two kinds of microphase separation structures exist in the process of liquid crystallization. In the POM pictures of Fig. 4b, two regions of fan-like structure and yellow/blue areas are observed at 76.8 and 75.7 °C, while at 55.0 °C only fan-like structure is found. The coexistence of two regions in the POM picture may correspond to two kinds of microphase separation structures. Although q_m and its intensity are plotted against the temperature in Fig. 7, it is noted here that such variation of the microphase separation structure is not necessarily temperature dependent but time dependent as shown in Fig. 8, namely it occurs in the *process* of liquid crystallization. Fig. 8a shows time dependence of POM picture for BLC44 quenched rapidly to 77.0 °C from the isotropic state. Two phases are observed in the initial stage, and then fan-like structure develops to cover the whole area. In the heating process from 77.0 °C (Fig. 8b), on the other hand, the fan-like structure disappears not through the way of the two phases. The same behavior is observed in Fig. 9, which shows the time-resolved SAXS profiles in heating and subsequent holding at 137.4 °C. The peak intensity at $q_m = 0.11\ nm^{-1}$ decreases around 133 °C and, in place of that, a new peak appears at $q_m = 0.17\ nm^{-1}$ which is the same position as the above one in the isotropic state. From these observations it is

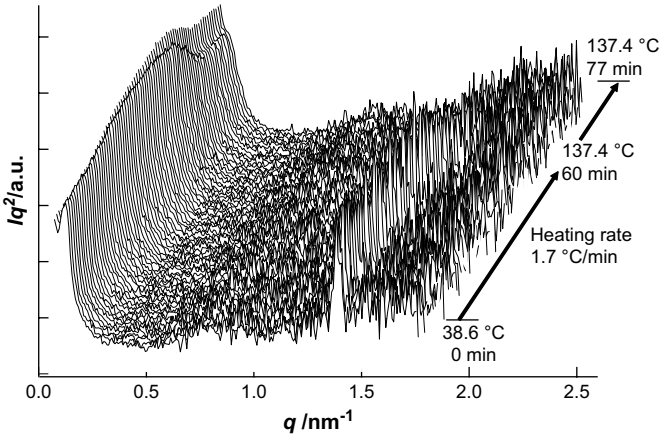

Fig. 9. Lorentz-corrected SAXS profiles for BLC44 in heating to 137.4 °C and subsequent holding at that temperature. Heating was performed after the cooling measurement shown in Fig. 6.

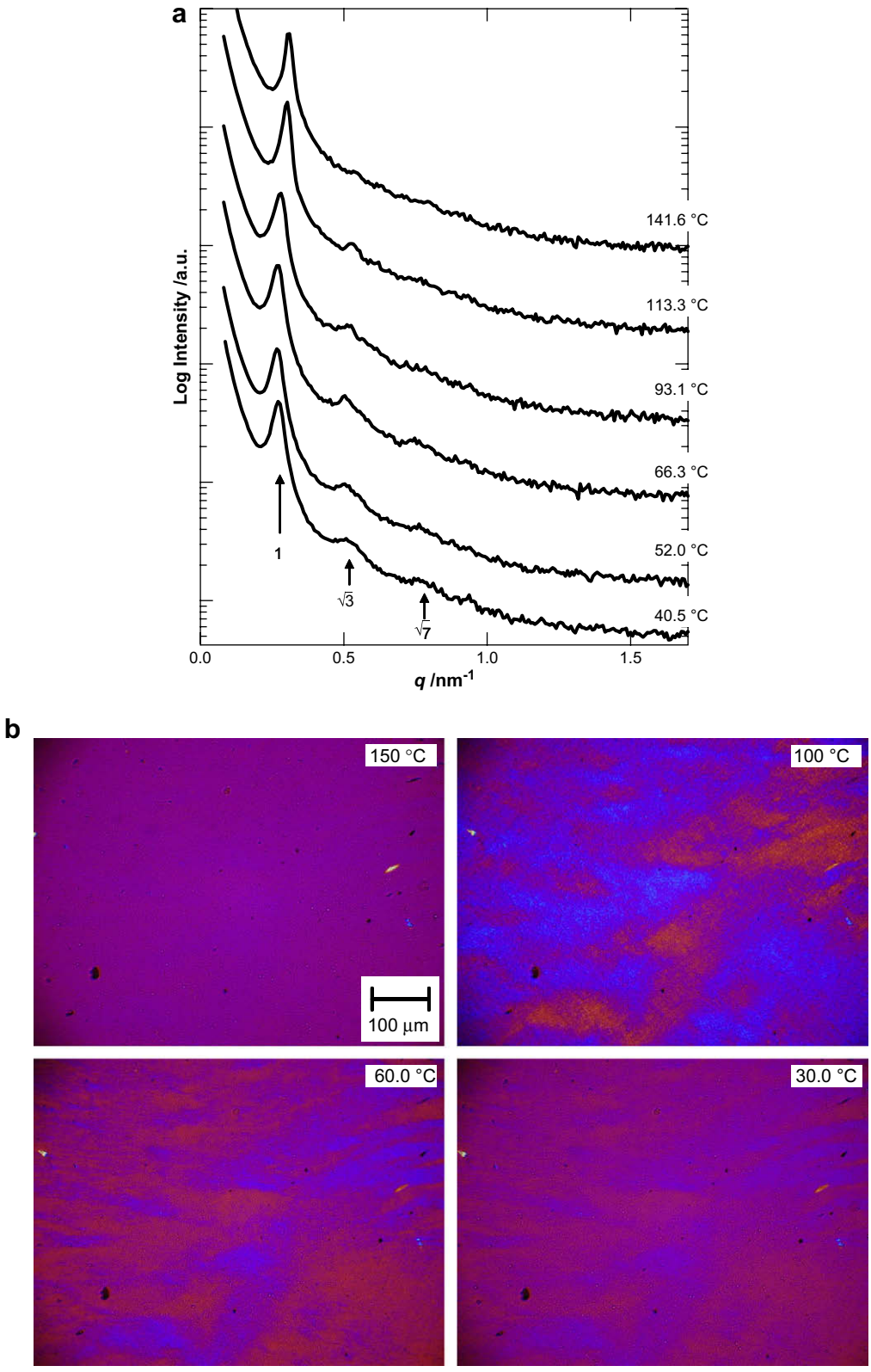

Fig. 10. SAXS profiles (a) and POM pictures (b) for BLC20 in cooling at 4 °C/min.

concluded that in the liquid crystallization process, two microphase separation structures (i.e., two liquid crystalline phases) appear first and then are reduced to one phase, while that the isotropization does not proceed through the way of two phases, but directly from one liquid crystalline phase. Furthermore, the change of the microphase separation structure in the liquid crystallization is discrete to Sm phase, and continuous to the other phase that disappears with the development of liquid crystallization.

Li et al. reported that the lamellar spacing was changed at the nematic–isotropic transition to be larger in the liquid crystalline

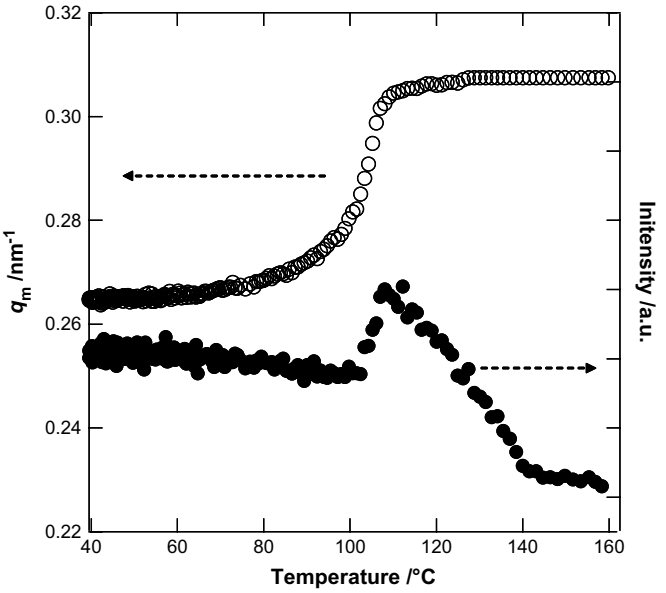

Fig. 11. Temperature dependences of the first-order peak position q_m and its intensity for BLC20.

state than in the isotropic state in the same way as our result, but the change of the spacing was continuous [10]. The discrete change has not been found so far, to our knowledge. For a main-chain polyester homopolymer, on the other hand, Tokita et al. [27] found an anisotropic domain development prior to the onset of the smectic layer ordering during the isothermal liquid crystallization from the isotropic phase at large supercooling. This suggests that the smectic layer structure is evolved through a transient nematic phase. Although our liquid crystalline polymer is a side-chain type and a component of the block copolymer, the behavior observed here that one more phase appears in the early stage of the liquid crystallization may be related to that found by Tokita et al., if that phase is nematic.

Fig. 10a shows SAXS profiles at selective temperatures in cooling from the isotropic state for BLC20. Although no peak is observed around $q = 1.4\ \mathrm{nm}^{-1}$ and no clear transition was detected in the DSC thermogram, liquid crystallization is considered to occur because some molecular orientations can be observed in POM pictures below about 110 °C as shown in Fig. 10b. These observations suggest that the liquid crystalline structure is not smectic but probably nematic. On the other hand, some peaks due to the microphase separation structure can be observed in a q range smaller than $1.0\ \mathrm{nm}^{-1}$. From the ratio of the higher-order peak positions to the first-order one, microphase separation structure is concluded to be cylindrical in both isotropic and liquid crystalline

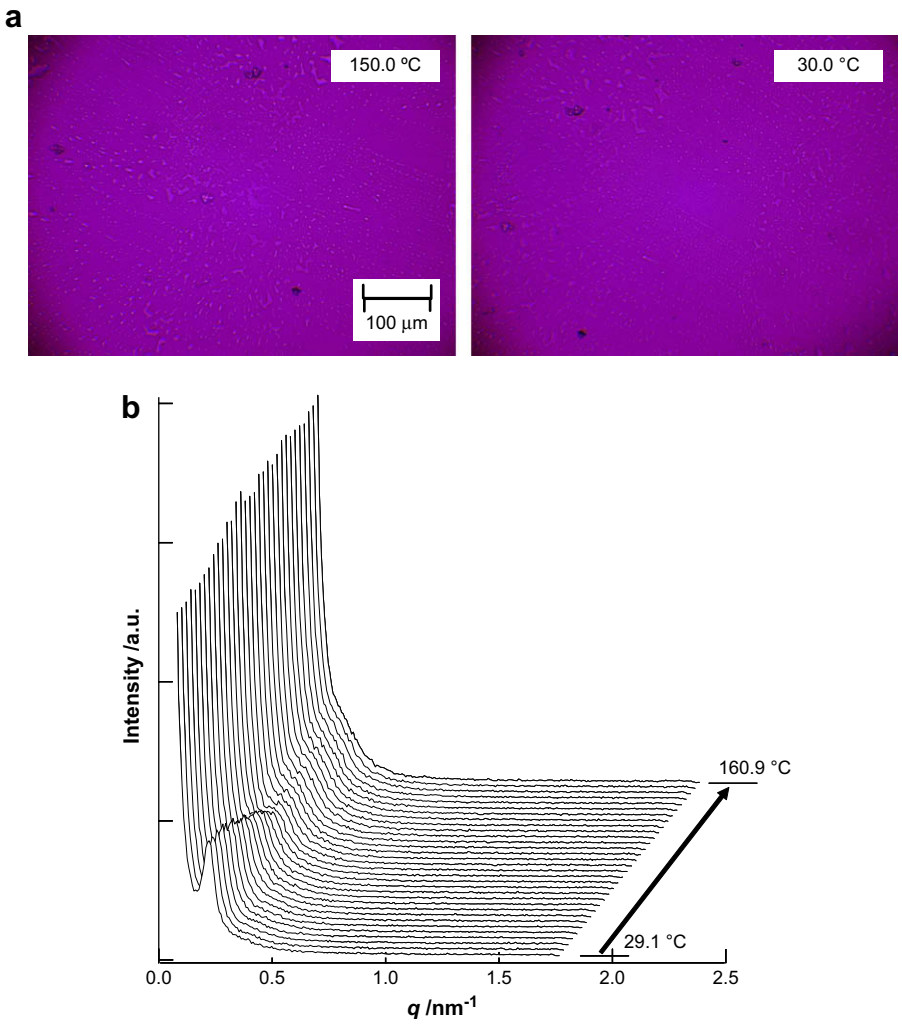

Fig. 12. POM pictures (a) and temperature dependence of SAXS profiles (b) for BLC15.

states, which suggests that liquid crystallization occurred within cylindrical domains.

In the liquid crystallization process, as shown in Fig. 11, BLC20 also has a change in both q_m and its peak intensity at about 110 °C: from $q_m = 0.31\ nm^{-1}$ (spacing: $d = 20.2$ nm) in the isotropic state to $0.266\ nm^{-1}$ ($d = 23.6$ nm) in the liquid crystalline state. From these values of d, the radii r of the cylinders in both states are estimated to be 5.5 and 6.4 nm, respectively, in the hexagonal packing when the volume fraction of the component is assumed to be the weight fraction. In this system, the change of q_m in the liquid crystallization may be continuous because the peak intensity does not decrease so much but just to the intensity in the liquid crystalline state. Two kinds of microphase separation structures were not seen in the liquid crystallization process. The change of q_m at the nematic–isotropic transition found by Li et al. was also continuous [10] as described above. The decrease in the peak intensity above 110 °C may come from the order–disorder transition whose temperature T_{ODT} may exist over 140 °C.

Fig. 12a shows POM pictures at selected temperatures for BLC15. Any structure due to molecular orientation is not observed even at a low temperature. In the SAXS profiles shown in Fig. 12b, no peak appears around $q = 1.4\ nm^{-1}$. The DSC thermogram showed no transition peak. These mean that no liquid crystallization occurs. The position, $q_m = 0.212\ nm^{-1}$, of the SAXS peak due to the microphase separation structure is not changed with temperature because of no liquid crystallization. Assuming that the domain of PLC block is spherical and that the volume fraction of the block equals to the weight fraction, the radius r is 7.74 nm in the bcc packing. Liquid crystallization may be impossible within the sphere with this size. Disappearance of the peak with increasing temperature in a higher temperature region may be due to the order–disorder transition (T_{ODT} = ca. 120 °C).

3.3. Phase structure in liquid crystalline state

Fig. 13 shows a 2D-SAXS profile for BLC51 measured immediately after applying shear to the sample. The orientation of the peaks due to the Sm layer is perpendicular to that of the intensity distribution in a smaller q range, which means that the Sm layer aligns perpendicularly to the interface between PBA and PLC lamellar domains. Anthamatten et al. investigated the orientation of Sm layers to microphase separation morphology for block copolymers consisting of amorphous polystyrene and methacrylate-based LC blocks [12]. According to their results, the orientation of the Sm layer within the lamellar domain is parallel to the interface for the block copolymers having a decyl spacer in the side group, while perpendicular for a hexyl spacer. Although their film samples were prepared by roll-casting, the orientation obtained by them is different from our result if decyl and undecyl spacers, used in their and our works, respectively, have the same effect on the orientation.

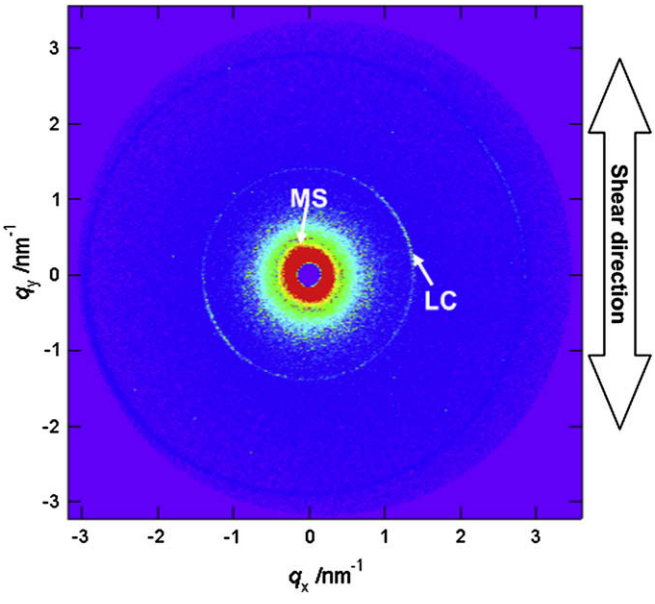

Fig. 13. 2D-SAXS image for BLC51 at 85 °C. MS and LC are due to microphase separation structure and Sm liquid crystalline structure, respectively.

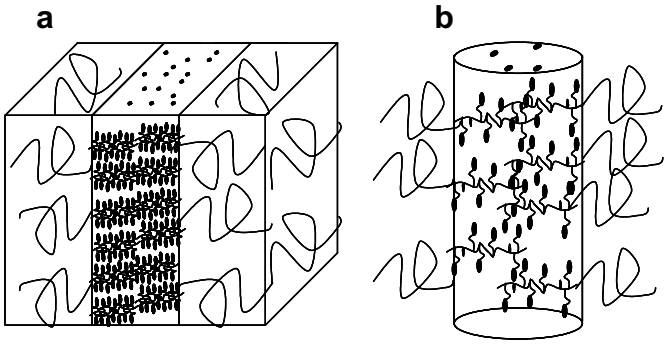

Fig. 14. Schematic models of orientation for lamellar/Sm structure (a) and cylindrical/nematic structure (b).

In Fig. 14a is shown a schematic model of the perpendicular orientation of Sm layers for BLC44. The spacing d of the lamellar microphase structure is 38 and 56 nm at 120 °C (in the isotropic state) and 40 °C (in the liquid crystalline state), respectively, as described in the previous section. Taking account of the copolymer composition (approximated to be weight fraction ≈ volume fraction), the thicknesses, d_{PLC} and d_{PBA}, of PLC and PBA lamellar domains are 16.7 and 21.3 nm, respectively, in the isotropic state. Assuming that d_{PBA} is not changed even in liquid crystallization, d_{PLC} is 34.7 nm in the liquid crystalline state. If the orientation of Sm layers is perpendicular, d_{PLC} may be somewhat smaller than 34.7 nm, because the PBA chain is expanded toward the lamellar interface, namely the PBA domain thickness becomes larger, to match the interface areas per junction of PBA and PLC blocks. Alternatively, when the lamellar thickness is taken to be proportional to the copolymer composition in the liquid crystalline state as well as in the isotropic state, d_{PLC} is 24.6 nm in the liquid crystalline state. Thus, the PLC lamellar thickness d_{PLC} may be in the range of 24.6–34.7 nm. On the other hand, the end-to-end distance of the fully extended PLC main chain with a *trans* zigzag conformation is estimated to be 18.2 nm on the basis of 71.6 of degrees of polymerization and 0.254 nm of C–C–C length per monomer. The difference between the above lamellar thickness d_{PLC} and twice the end-to-end distance of the fully extended PLC main chain is not so large. Namely the PLC main chain must be considerably extended toward the lamellar interface in the perpendicular alignment of Sm layers.

For BLC20, although there is no experimental evidence, the orientation of the mesogenic groups in the nematic alignment may be parallel to the cylinder axis as shown in Fig. 14b, as pointed out by Mao et al. [7].

4. Conclusion

Phase behavior in liquid crystallization was investigated for diblock copolymers having rubbery amorphous and side-group liquid crystalline components.

In the liquid crystallization from the lamellar microphase separation structure, the liquid crystalline structure was smectic in the same way as PLC homopolymer. In the process of the liquid crystallization, the intensity of the SAXS peak due to the preexisting microphase separation structure decreased and the peak position was changed continuously to a smaller angular side. At almost the same time, a new peak appeared at a further smaller q and developed. The former peak disappeared with proceeding of the liquid crystallization. The behavior of these SAXS peaks suggests that the microphase separation structure was changed discretely at the transition from isotropic to smectic and that two phases coexist in the early stage of the liquid crystallization. In the isotropization, coexistence of two phases observed in the liquid crystallization was not observed.

The liquid crystallization within cylindrical microphase domains does not give smectic but probably nematic structure. A change in the spacing of the microphase separation structure was observed in the liquid crystallization process, but it was a continuous change in the same way as reported by Li et al. [10] for the nematic–isotropic transition.

The block copolymer with a 15 wt% LC composition gave no liquid crystallization. Assuming the spherical structure in this block copolymer, the radius of the sphere domain is 7.7 nm. This sphere size is considered not to be enough for liquid crystallization, taking account of the size of the side group and the spacing of Sm layers.

The orientation of Sm layers within the lamellar domain was concluded from the 2D-SAXS measurements to be perpendicular to the lamellar interface, which is different from that obtained by Anthamatten et al. [12] if the decyl and undecyl spacers have the same effect on the orientation. In the perpendicular alignment, the PLC main chain should be extended toward the interface, compared with the lamellar thickness.

Acknowledgements

This work was supported by Grants in Aid for Scientific Research on Basic Areas (B) (18350114) from Japan Society for the Promotion of Science and by the 21st Century COE Program for Scientific Research from the Ministry of Education, Culture, Sports, Science and Technology. The SAXS experiments using synchrotron radiation were performed under the approval of the Photon Factory Program Advisory Committee (Proposal Nos. 2004G090, 2006G087 and 2007G090).

References

[1] Fischer H, Poser S, Arnold M, Frank W. Macromolecules 1994;27:7133–8.
[2] Wang J, Mao G, Ober CK, Kramer EJ. Macromolecules 1997;30:1906–14.
[3] Kasko AM, Heinz AM, Pugh C. Macromolecules 1998;31:256–71.
[4] Anthamatten M, Wu JS, Hammond PT. Macromolecules 2001;34:8574–9.
[5] Kasko AM, Grunwald SR, Pugh C. Macromolecules 2002;35:5466–74.
[6] Hamley IW, Castelletto V, Parras P, Lu ZB, Imrie CT, Itoh T. Soft Matter 2005;1:355–63.
[7] Mao G, Wang J, Clingman SR, Ober CK, Chen JT, Thomas EL. Macromolecules 1997;30:2556–67.
[8] Zheng WY, Albalak RJ, Hammond PT. Macromolecules 1998;31:2686–9.
[9] Yamada M, Itoh T, Nakagawa R, Hirao A, Nakahama S, Watanabe J. Macromolecules 1999;32:282–9.
[10] Li MH, Keller P, Albouy PA. Macromolecules 2003;36:2284–92.
[11] Ansari IA, Castelletto V, Mykhaylyk T, Hamley IW, Lu ZB, Itoh T, et al. Macromolecules 2003;36:8898–901.
[12] Anthamatten M, Zheng WY, Hammond PT. Macromolecules 1999;32:4838–48.
[13] Hamley IW, Castelletto V, Lu ZB, Imrie CT, Itoh T, Al-Hussein M. Macromolecules 2004;37:4798–807.
[14] Tomikawa N, Lu Z, Itoh T, Imrie CT, Adachi M, Tokita M, et al. Jpn J Appl Phys 2005;44:711–4.
[15] Anthamatten M, Hammond PT. Macromolecules 1999;32:8066–76.
[16] Al-Hussein M, Séréro Y, Konovalov O, Mourran A, Möller M, de Jeu WH. Macromolecules 2005;38:9610–6.
[17] Tokita M, Adachi M, Masuyama S, Takazawa F, Watanabe J. Macromolecules 2007;40:7276–82.
[18] Hamley IW. The physics of block copolymers. New York: Oxford; 1998 [chapter 5].
[19] Huang P, Zhu L, Guo Y, Ge Q, Jing AJ, Chen WY, et al. Macromolecules 2004;37:3689–98.
[20] Takeshita H, Ishii N, Araki C, Miya M, Takenaka K, Shiomi T. J Polym Sci Part B 2004;42:4199–206.
[21] Takeshita H, Gao YJ, Natsui T, Rodriguez E, Miya M, Takenaka K, et al. Polymer 2007;48:7600–71.
[22] Nojima S, Kato K, Yamamoto S, Ashida T. Macromolecules 1992;25:2237–42.
[23] Quiram DJ, Register RA, Marchand GR, Ryan AJ. Macromolecules 1997;30:8338–43.
[24] Shiomi T, Takeshita H, Kawaguchi H, Nagai M, Takenaka K, Miya M. Macromolecules 2002;35:8056–65.
[25] Ueki T, Hiiragi Y, Kataoka M, Inoko Y, Amemiya Y, Izumi Y, et al. Biophys Chem 1985;23:115–24.
[26] Kostromin SG, Shibaev VP. Polym Sci Ser B 1999;41:346–58.
[27] Tokita M, Kim K-W, Kang S, Watanabe J. Macromolecules 2006;39:2021–3.